Novel Small-Size Directional Antenna for UWB WBAN/WPAN Applications

Maciej Klemm, *Student Member, IEEE*, István Z. Kovács, *Member, IEEE*, Gert F. Pedersen, *Member, IEEE*, and Gerhard Tröster, *Senior Member, IEEE*

***Abstract*—This paper presents a novel small-size directional antenna design for ultrawide-band wireless body area networks/wireless personal area networks applications. The design is based on a typical slot antenna structure with an added reflector in order to achieve directionality. The effects of different antenna parameters and human body proximity on the radiation characteristics are analyzed. Antenna measurements with an optic RF setup were performed in order to characterize the small-size antenna far field radiation pattern. The different structural antenna parameters were optimized via extensive numerical simulations. Results show that for frequencies above 3.5 GHz, where the power front-to-back ratio of the directional antenna is greater than 10 dB, its impedance is nearly the same as in the free space. It is not the case neither for the omnidirectional slot antenna nor the monopole antenna next to the body. Between 3 and 6 GHz performance of the novel directional antenna, in terms of radiation efficiency and SAR values, is significantly improved compared to omnidirectional antenna designs.**

***Index Terms*—Body-worn antennas, human body, pulsed antennas, specific absorption rate (SAR), ultrawide-band (UWB), wearable antennas, wireless communication.**

I. Introduction

In the past few years ultrawide-band (UWB) technology has received increasing attention in the wireless world. Its main envisioned advantages over conventional (narrowband) wireless communications systems are: low transmit power levels, high-data rates, and possibly simpler hardware configurations. Wireless personal area networks (WPAN) and wireless body area networks (WBAN) are seen as one of the major fields where such UWB characteristics can be potentially exploited [1]–[4]. Antennas play a critical role in the UWB communication systems, since they act as pulse-shaping filters [5]. In impulse radio based UWB systems (TH-UWB, DS-UWB) the antenna performance and characteristics influence the design of the pulse generator and also the complexity of the detection mechanism in the receiver [6]. For any UWB antenna, the flat frequency response requirement in a given band cannot be obtained for all spatial directions [7]. Generally, there can be only a limited area/direction in which the nondispersive conditions are well approximated [8], thus the impulse response of the antenna becomes an additional design parameter. The choice for a specific UWB antenna design has to be based on the main implementation requirements. As we will show later in this paper, this aspect is especially important in the UWB WBAN/WPAN applications. They require that antennas must have small form factor (esp. in WBAN), good efficiency, easy integration with circuitry and good transient characteristics (short impulse response). There are several UWB antenna designs available, which meet some of the imposed requirements [9]–[11]. Additional requirements exist for UWB WBAN antennas, since the proximity of the human body can significantly modify their impedance bandwidth and radiation characteristics, thus modifying also the transient characteristics of the antenna [13]. These main observations have led us to the conclusion that for an efficient design the UWB antennas used in WBAN/WPAN devices have to be designed and tested in their normal operating scenarios. However, very few UWB antenna designs concerned with this issue were reported in open literature, both for WPAN [12] and WBAN [13], [15] applications.

Most of the antenna designs presented so far for UWB WPAN/WBAN, present radiation patterns similar to the traditional monopole/dipole antennas. However, a directional radiation pattern of an antenna would be desirable for body-worn devices (WBAN) in order to minimize the effects of the human body proximity and body exposure to EM radiation. To obtain this, the radiation toward the body needs either not to take place or to be minimized. Generally, directivity can be obtained if the antenna is large in the direction of interest, such as horn or Vivaldi antennas [16]. Other ways to achieve directional antenna pattern include adding the cavity or shielding plane behind the antenna, or using the absorbing materials [17]. However these techniques lead to either serious increase in a size of an antenna, a more complicated manufacturing or a decreased efficiency. As it was shown in [18], [19], another way to reduce the backward radiation is incorporation of reflecting element. However this method has been used [18], [19] only to improve the front-to-back ratio of antennas, which were already directional (with a front-to-back ratio >10 dB). Introduction of a reflecting element had therefore negligible effect on the input impedance of the antenna and the reflector could be safely incorporated into existing design. The size of the antenna was also not an issue for the investigations presented in [18], [19].

In this paper we propose a novel small-size directional antenna for UWB systems, with the main focus on the WBAN (body-worn) applications. It is based on the omnidirectional UWB slot antenna design (presented also in this paper) and utilizes the reflecting patch element to achieve front-to-back ratio

Manuscript received March 22, 2005; revised July 9, 2005.

M. Klemm and G. Tröster are with the Electronics Laboratory of the Department of Information Technology and Electrical Engineering, Swiss Federal Institute of Technology (ETH) Zürich, 8092 Zürich, Switzerland (e-mail: klemm@ife.ee.ethz.ch).

I. Z. Kovács and G. F. Pedersen are with the Antennas and Propagation Laboratory of the Department of Communication Technology, Aalborg University, Niels Jernes Vej 12, Aalborg, Denmark (e-mail: {istvan, gfp}@kom.auc.dk).

Digital Object Identifier 10.1109/TAP.2005.859906

better than 10 dB across a wide frequency range (in far field). By means of the full-wave electromagnetic (EM) numerical FIT method (using commercial CST Microwave Studio), a systematic parameter study of our new design was performed to investigate the influence of the reflector and other antenna parameters on transient characteristics of the new antenna. Further analysis incorporated the human body models in a WBAN operating scenario. Moreover, a *true* characterization of UWB antenna is presented based on the antenna transfer function.

The paper is organized as follows: In Section II, the parameters used for UWB antenna characterization and source pulse are presented. In Section III we show the special cable-less measurement set-up, suitable for electrically small antenna measurements. This section also introduces human body models used during numerical electromagnetic simulations. To provide a reference for results obtained with the new antenna design a commonly known/used example of small UWB antenna, the disc monopole antenna is presented in Section IV. Section V presents the design of an omnidirectional UWB slot antenna, supported by a very small ground plane size, as well as the design and characterization of a new directional UWB slot antenna. Spatial UWB characteristics (averaged transfer functions and pulse distortions) are analyzed in Section VI, for two different directional antennas and omnidirectional antennas, when operating in the free space. Finally, the influence of the human body on different designs (examining radiation efficiency, impedance and averaged transfer functions) is shown in Section VII.

II. Parameters Used for UWB Antennas Characterization

A very wide operational bandwidth of UWB systems makes the design and evaluation of antennas much more difficult. For the same reason traditional narrowband parameters characterizing antenna, such as return loss, radiation pattern, polarization are relatively less useful for UWB radio systems. Therefore UWB antennas should be evaluated by means of different parameters,such as the antenna transfer function (TF). Together with the waveform driving the antenna TF allows distortions introduced by the UWB antenna to be calculated. In the following sections we will base the antenna design and evaluation on the following parameters.

A. 'Narrowband' Parameters

As it was mentioned, even if not directly useful, parameters known from the traditional (narrowband systems) antenna theory can be helpful. In our investigations we were looking at the return loss parameter, as it is also the part in the antenna transfer function. In further investigation the impedance bandwidth is defined as $|S_{11}| < -10$ dB. We were also looking at the radiation patterns on different frequencies, by which we can (only) roughly estimate the behavior of the transfer functions in different propagation directions. The 3-D radiation patterns were used to calculate the antenna front-to-back (F2B) ratio, defined as a ratio of total power radiated in the two half-spaces in the far field.

B. Source Pulse

As a source pulse we have used the Gaussian modulated pulse, which has the following form:

$$s(t) = e^{-\left(\frac{t}{\tau}\right)^2} \cdot cos(2\pi f_r \cdot t) \tag{1}$$

where f_r defines center frequency of the pulse, τ (natural pulse width) defines its bandwidth. Based on the amplitude characteristics of transfer functions of investigated antennas (see Section V), we have chosen $f_r = 5$ GHz and $\tau = 160$ ps. It gives the -10 dB pulse bandwidth from approximately 3 to 7 GHz.

C. Frequency Domain Transfer Functions

During the design of the new antenna we have investigated transmit (Tx) transfer function defined as [20]

$$\mathcal{H}_{Tx}(\omega, \theta, \phi) = \frac{E_{\mathrm{rad}}(\omega, \theta, \phi)}{V_{\mathrm{in}}(\omega)} \tag{2}$$

It relates the radiated electric field intensity E_{rad} and the pulse from the generator V_{in} driving the antenna. This definition is very convenient for practical cases, because it also includes the impedance match between the antenna and the pulse generator. In this form H_{Tx} is easily computable from the time-domain electromagnetic solvers, applying Fourier transformation.

D. Spatially Averaged Transfer Functions

We introduce a new parameter for UWB antenna characterization—the spatially averaged transfer function, expressed as

$$H_{av}(\omega, \Omega) = \frac{\sum_{n=1}^{N} \sum_{m=1}^{M} H_{\mathrm{norm}}(\omega, \Delta\omega, \theta_n, \phi_m)}{N \cdot M} \tag{3}$$

where H_{norm} are the transfer functions in a given direction, normalized to the maximum value within the frequency band $\Delta\omega$. $N$and M are propagation directions for the θ and ϕ coordinate, respectively. The choice for the $\Delta\omega$ should be based on the spectrum of the antenna input pulse. H_{av} is a very useful parameter and can be calculated for different solid angles $(\Omega \in (\theta_n, \phi_m))$ of the radiation sphere, or for the entire sphere, depending on the interest. Preferable directions of propagation with best performance in terms of transient characteristics could be found for a given antenna as well. Concept of H_{av} parameter is similar to the mean effective gain (MEG) [21] or mean effective energy gain [22], however it deals with the frequency-dependant transfer function (which is more appropriate to characterize UWB antennas).

E. Pulse Distortion Parameters

Based on the transfer functions we are able to calculate pulse distortions introduced by an antenna. For UWB systems, the commonly used receivers are based on the pulse energy detection or correlation with the template waveform. Therefore we will examine the pulse distortions by calculating fidelity factor and time spread of radiated pulses (with respect to the antenna

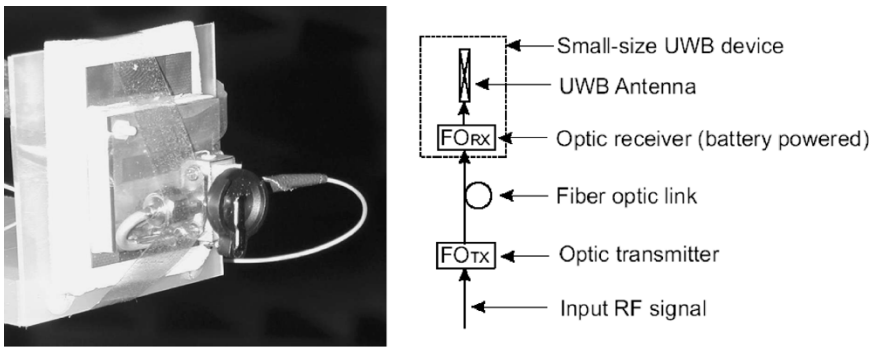

Fig. 1. Small-size antenna measurement setup using RF on fiber optic: (a) photo of the antenna measurement setup (antenna, optical receiver and fiber link) and (b) block diagram of the RF on fiber optic setup.

input pulse). Fidelity between waveforms $x(t)$ and $y(t)$ is generally defined as

$$F = max \frac{\int_{-\infty}^{\infty} x(t) \cdot y(t-\tau) dt}{\sqrt{\int_{-\infty}^{\infty} |x(t)^2|\, dt \cdot \int_{-\infty}^{\infty} |y(t)^2|\, dt}}. \quad (4)$$

The fidelity parameter F, is the maximum of the cross-correlation function and compares only shapes of both waveforms, not amplitudes. Time spread is a ratio between the lengths of the 99% energy window (E99) of the radiated pulse and the antenna input pulse (source pulse). It discloses how much the energy of radiated pulse is spread compared to the input pulse.

III. Measurement and Simulation Setup

A. Antenna Measurement Setup

In traditional antenna measurements, the antenna is connected to the measurement equipment with a coaxial cable. This set-up is perfectly suited for electrically large antennas, but not for electrically small antennas, as the radiation characteristics are significantly influenced by the size of the ground plane or any conductive cables acting as additional ground planes [14], [15]. The influence of the connecting feed cables or any other conductive cables connected to the device, which does not belong to the final application, ought to be minimized if not completely eliminated. In [14], [15] a practical set-up was proposed to achieve this, namely the use of an RF on fiber optic (FO) link (transmitter and receiver) instead of the usual conductive cable feed connections. Fig. 1 shows the RF on fiber optic setup used in our antenna measurements.

The comparison between measured and simulated radiation patterns are presented in Fig. 2, for the two principal planes, at 3.5, 4.5, and 6 GHz. Good agreement is achieved, especially for the co-polarization component. In the final application the transmitter (pulse generator) will be integrated on the antenna, so we expect the radiation characteristics very close to simulated of the directional antenna (see Section VI), without any additional cables or metallic elements.

B. Human Body Models for Numerical Electromagnetic Simulations

In the main applications (UWB WBAN) the antenna is mounted on the human body. It is known that the body has a significant impact on the antenna characteristics (radiation pattern, efficiency and input impedance). Therefore, it is important to include the human body in the EM simulations. We have included two different models of the human body. The first one is a three-tissue model, consisting of layers of skin (1-mm thick), fat (3-mm thick) and a muscle tissue (40-mm thick), and the second is a simple homogeneous model composed of muscle tissue (44-mm thick). Overall dimensions of these models are the same: $120 \times 110 \times 44$ mm^3. The size of this truncated body model was found by comparing the simulation results in terms of antenna radiation characteristics when a larger (by 50%) model was used. No significant differences were noticed. The human tissues are dispersive and their electrical properties are therefore changing over frequencies. The influence of these changes on the antenna characteristics was investigated by an EM code which could include frequency dispersion and it was found to have a minor influence (e.g., radiation efficiency changes <5%), thus in all further investigations the electrical parameters of the tissues were assumed to be nondispersive and the values as at the centre frequency (4.5 GHz) were used [25]: skin-$\epsilon_r = 38$, $\sigma = 2.7$ [S/m]; fat-$\epsilon_r = 5.1$, $\sigma = 0.18$ [S/m]; muscle-$\epsilon_r = 50.8$, $\sigma = 3$ [S/m].

IV. Reference Antenna Design- UWB Disc Monopole

Different kinds of monopole antennas are very often used in UWB applications and we have therefore included results for a UWB monopole antenna as reference. We designed the UWB disc monopole, with the criteria of an impedance bandwidth from 3 to 6 GHz ($|S_{11}| < -10$ dB) and with the size comparable to the of slot antenna. The antenna geometry is shown in Fig. 3(a). Its dimensions are: ground plane $\mathrm{G}_W = \mathrm{G}_L = 20$ mm, disc diameter $\mathrm{D} = 16$ mm. Gap between ground plane and disc is 0.75 mm. Overall planar dimension of antenna is 36.75×20 mm. It was realized on a 0.5-mm thick FR4 substrate ($\epsilon_r = 4.4$) and is fed from a 50 Ω microstrip line.

It is relatively easy to design a UWB monopole antenna when considering only the impedance bandwidth. But to achieve the same radiation pattern bandwidth is difficult, due to the significant changes in the antenna pattern at higher frequencies [26]. Plots of the return loss and the H_{Tx} function (in $\theta = 0$, $\phi = 0$ direction) of the UWB disc monopole antenna are shown in Fig. 3(b). As can be seen, the antenna is well matched in a much

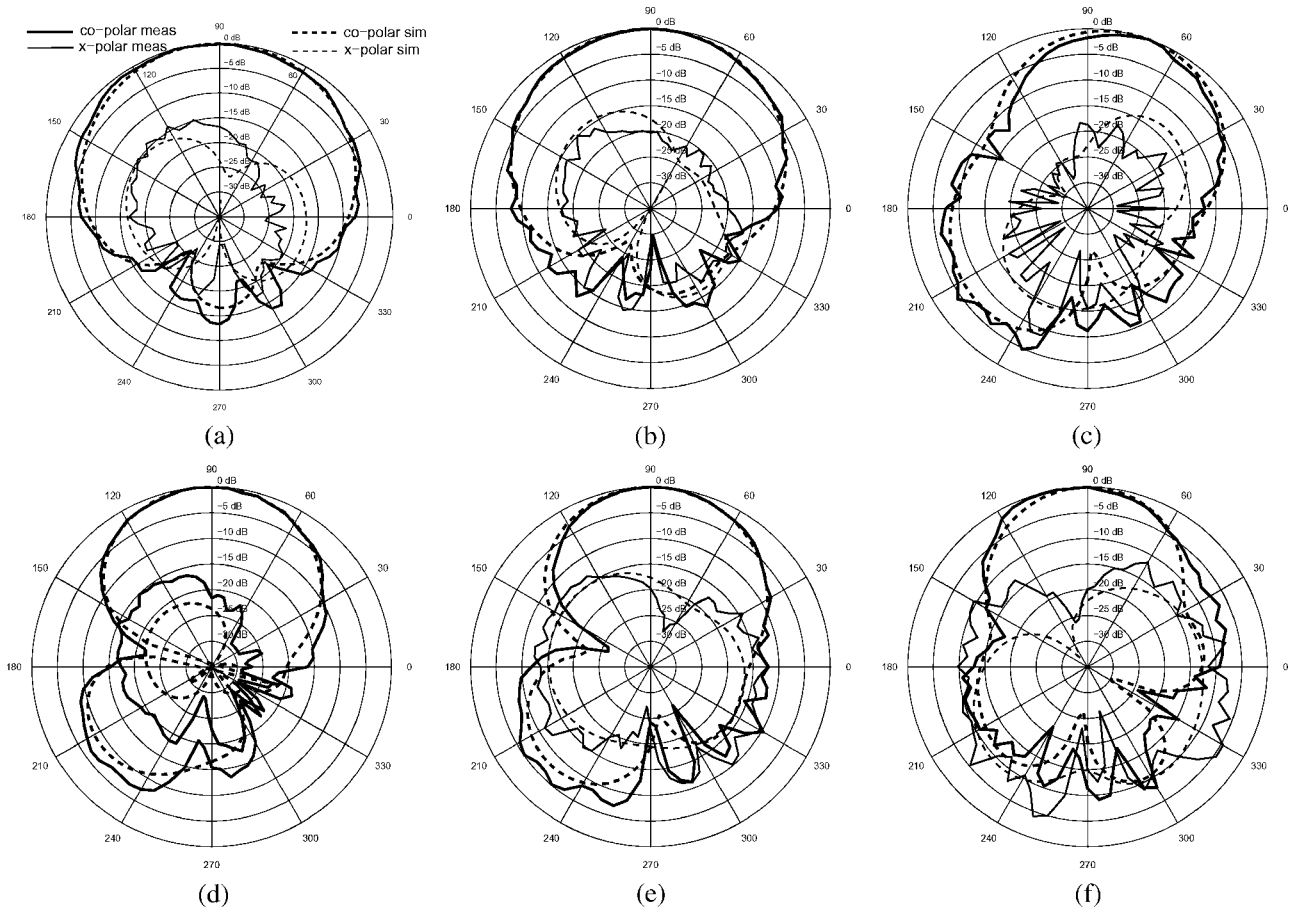

Fig. 2. Comparison of measured and simulated radiation patterns of directional slot antenna [see Fig. 1(a)]. (a) XZ plane 3.5 GHz, (b) XZ plane 4.5 GHz, (c) XZ plane 6 GHz, (d) YZ plane 3.5 GHz, and (e) YZ plane 4.5 GHz, (f) YZ plane 6 GHz.

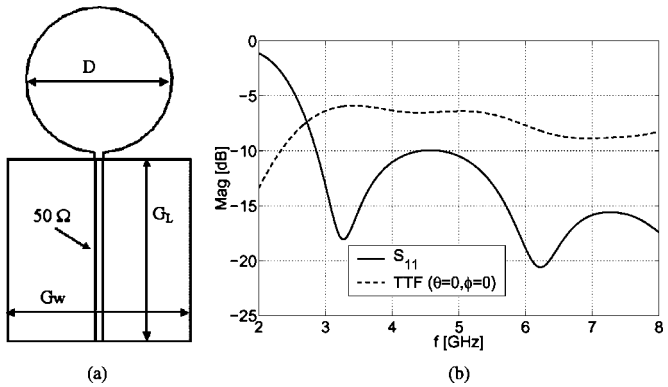

Fig. 3. UWB disc monopole antenna: (a) geometry of the antenna and (b) return loss and Tx transfer function (in propagation direction $\theta = 0$, $\phi = 0$).

wider bandwidth than 3–6 GHz. H_{Tx} is presented on the same scale as for different slot antennas from Fig. 5(b). It shows a weak integrative characteristic.

V. Small-Size Directional UWB Slot Antenna Design

The main objective of this work was to design an ultra wideband directional antenna, which is compact especially concerning the thickness of the antenna. The geometry of the proposed antenna is shown in Fig. 4.

As a first step the slot antenna without the reflector and on the small ground plane was designed. The antenna is a slot cut in the ground plane, fed by two symmetrically placed 100 Ω microstrip lines which are connected in parallel to the 50 Ω feed line. This feeding topology provides very wideband matching for slot and stacked patch antennas [23], [24]. Since our final application, a wearable UWB transmitter, will operate in the lower FCC UWB band (3–6 GHz), we achieved impedance bandwidth ($S_{11} = -10$ dB) of 67%. This is one of the widest bandwidths reported in the literature, for the medium width slot antenna. Moreover, it is realized on a very small ground plane. The overall antenna dimensions are defined by the ground plane size—32 × 29 mm ($0.32\lambda \times 0.29\lambda$ at the lowest operating frequency 3 GHz). Due to the small ground plane dimensions compared to the slot dimensions, the antenna has a quasiomni directional radiation pattern in an XZ plane. Moreover the antenna radiates almost the same amount of the power in the two half-spaces. Front-to-back ratio is 0.09, 0.44, and 0.72 dB at 3.5, 4.5, and 6 GHz, respectively.

To improve the front-to-back ratio we have added another radiating (reflecting) element below the feed line.

As has been shown [18], [19], this is an efficient way to reduce the backward radiation. However authors of [18], [19] have used this method only to improve front-to-back ratio of antennas, which were already directional (with a front-to-back ratio >10 dB). Introduction of a reflecting element therefore

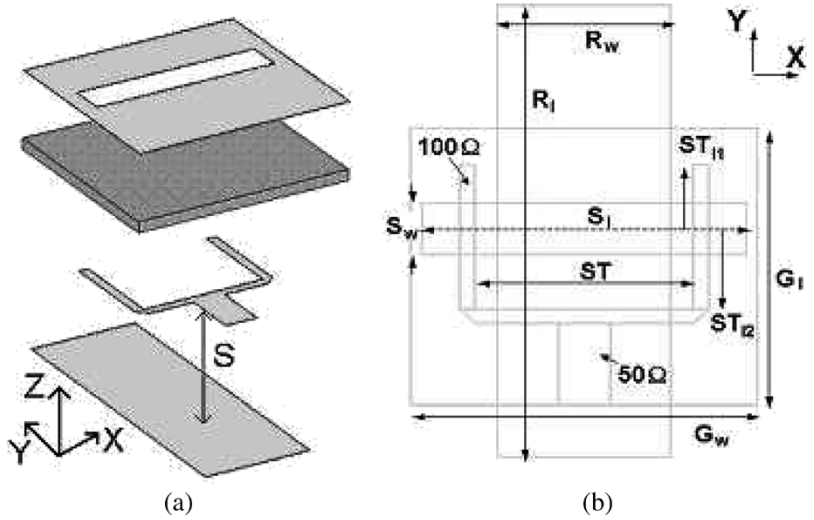

Fig. 4. Geometry of the novel small directional UWB antenna.

had negligible effect on the input impedance of the antenna and reflector could easily be incorporated into existing designs. This is certainly not our case, since we are dealing with the omnidirectional slot antenna. Due to the application requirements (WBAN, WPAN) we are interested in a very small spacing (<10 mm) between the reflector and the antenna feed line, to keep the antenna thickness as small as possible. Thus the input impedance of the antenna will be strongly influenced by the reflector. Further, the radiation properties of the new structure can not be analyzed in the same way as in [18], [19], where the design process involves examining the relative magnitude and phase of the radiated far field due to the slot and reflector (with desired solution of equal magnitudes and a 180^0 phase difference). To understand the influence of different antenna (slot antenna plus reflector) parameters on its impedance bandwidth and radiation characteristics, a systematic parametric study was performed. Table I presents initial design parameter of the directional UWB antenna, selected after several EM simulations, and dimensions of the omnidirectional UWB slot antenna. It should be noticed that since the reflector significantly affects antenna characteristics, values from Table I are different from those optimized for a single slot antenna. In our study one design parameter at the time was varied, keeping the others constant. For different antenna parameters we have investigated matching bandwidth (defined as $|S_{11}| < -10$ dB), radiation patterns at 3.5, 4.5, and 6 GHz and a transmit transfer function $H_{Tx}(\omega, 0, 0)$.

TABLE I
INITIAL DESIGN PARAMETERS OF THE ANTENNA SHOWN IN FIG. 4

Antenna parameters	*Directional antenna*	*Omni − directional antenna*
Slot length (S_l)	30mm	27.2mm
Slot width (S_w)	5mm	5mm
Reflector length (R_l)	44mm	-
Reflector width (R_w)	16mm	-
Ground plane width (G_w)	32mm	32mm
Ground plane length (G_l)	27mm	29mm
Microstrip feed line impedance	50Ω (4.8mm)	50Ω (4.8mm)
Microstrip tuning stubs impedance	100Ω (1.4mm)	100Ω (1.4mm)
Tuning stubs spacing (ST)	20.2mm	18.2mm
Tuning stubs length (ST_{l1})	6.15mm	6.15mm
Tuning stubs length (ST_{l2})	7.85mm	7.85mm
Reflector-feedline spacing (S)	6mm	-
Substrate material	ϵ_r=2.2	ϵ_r=2.2
Substrate material thickness (h)	1.58mm	1.58mm

A. Variation of the Spacing Between the Reflector and Feed Line (S)

Fig. 5(a) and (b) shows, the $|S_{11}|$ and $|H_{Tx}|$, respectively, for different S values (6, 8, 10 mm) and also without reflector (omnidirectional pattern). A very wide impedance bandwidth of 67% (3–6 GHz) for the slot antenna without reflector was achieved. With the addition of a reflector the shift in the impedance bandwidth is visible, especially at lower frequencies. Impedance bandwidth is 47% when the reflector is 6 mm away from the feed line, from 4 to 6.5 GHz. Moving the reflector further away keeps almost the same relative bandwidth (47% for 8 mm, 40% for 10 mm), but at the lower frequencies.

In Fig. 6 we can see the radiation patterns in two major planes at 3.5, 4.5, and 6 GHz, for different S values and also for the antenna without the reflector. The slot antenna radiates equal power in two hemispheres, with the gain increasing from 3.5 dB at 3.5 GHz to 5.3 dB at 6 GHz. With the presence of the reflector the front-to-back (F2B) ratio greatly increases, being above 10 dB for all S values (it varies slightly for different S values, but no more than 1 dB). As expected the gain of the antenna increases to around 7, 7.5 and 8.5 dB at 3.5, 4.5 and 6 GHz, respectively. Gain variations are not higher than 0.4 dB for different S values. It is also worth to notice, that the new directional antenna has a very stable radiation pattern across the frequency band of interest. In Fig. 5(b) we can see $|H_{Tx}(\omega, 0, 0)|$ characteristics. As visible, the omnidirectional slot antenna has very flat amplitude of H_{Tx}, with a 3 dB bandwidth from 2.85 to 8 GHz (95%). For directional antennas the amplitude of H_{Tx} has narrower bandpass characteristic, with a 3 dB bandwidth from around 3.5 to 7 GHz (67%). As expected the amplitude of H_{Tx} for the directional antenna is higher compared to the slot antenna, even at frequencies, where the matching is poor this

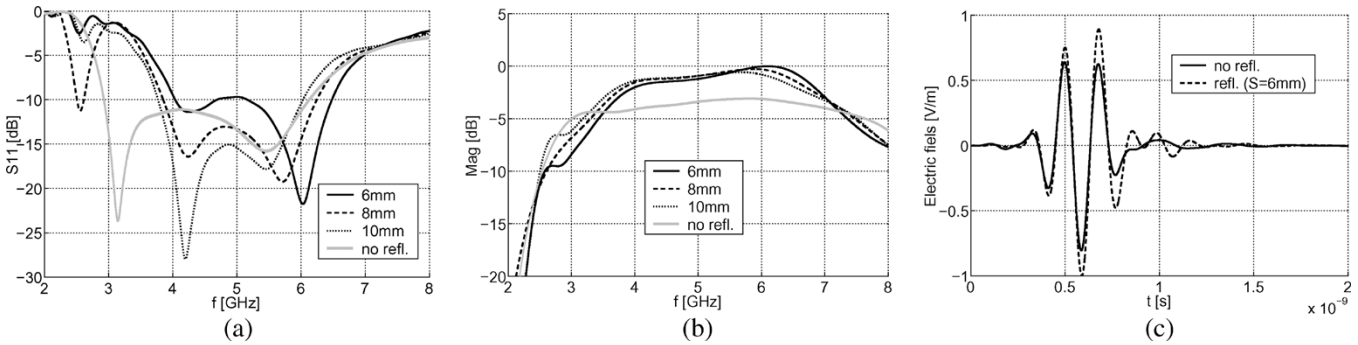

Fig. 5. (a) $|S_{11}|$ for different S, (b) $|H_{Tx}(\omega, 0, 0,)|$ transfer function for different S (curve named "no refl." corresponds to the slot antenna without reflector), and (c) radiated waveforms from the directional antenna (as in Table I) and from the slot antenna.

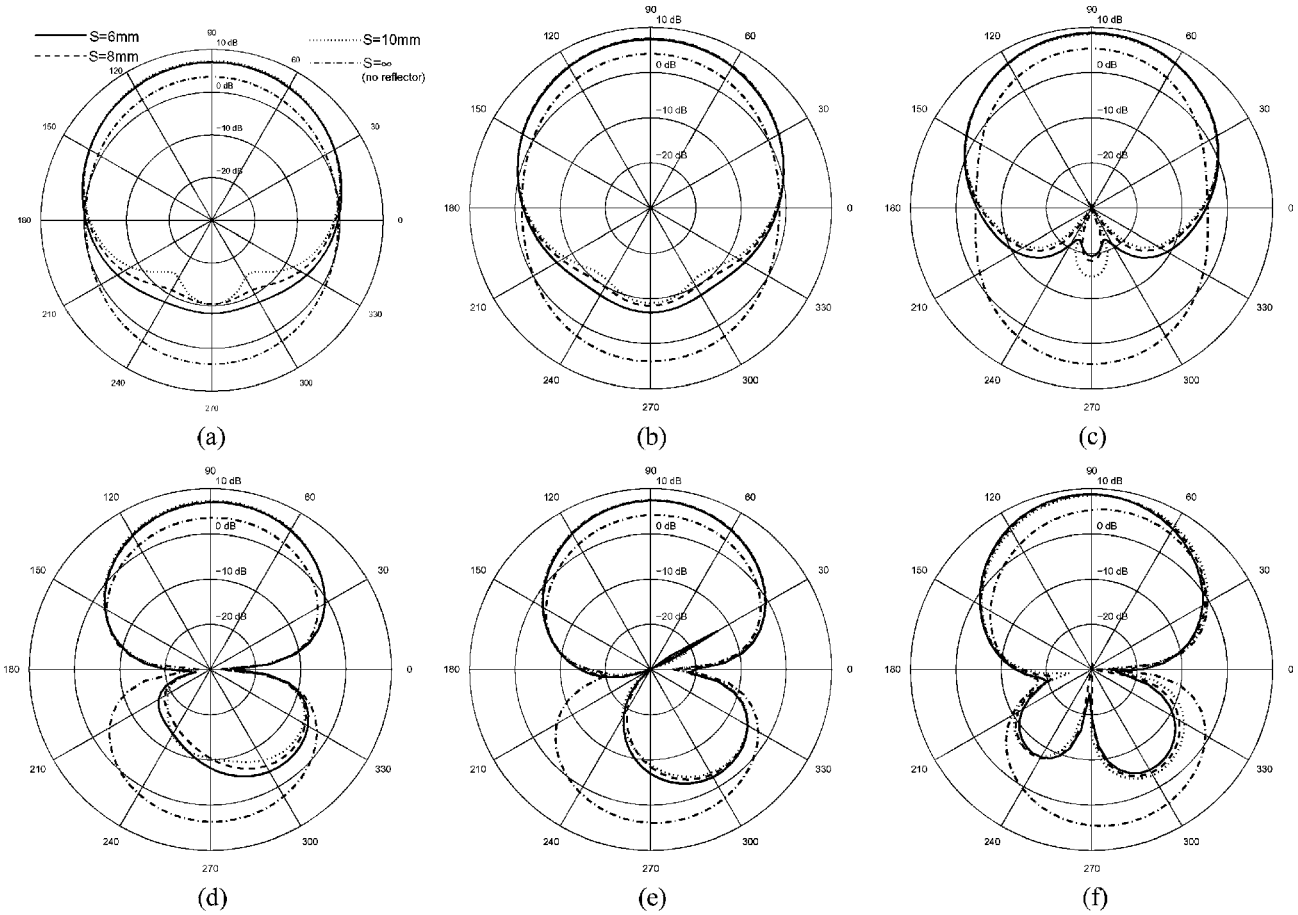

Fig. 6. Radiation patterns of directional slot antenna for different S. (a) XZ plane 3.5 GHz, (b) XZ plane 4.5 GHz, (c) XZ plane 6 GHz, (d) YZ plane 3.5 GHz, (e) YZ plane 4.5 GHz, and (f) YZ plane 6 GHz. Pattern of the omnidirectional slot antenna ($S = \infty$) included for comparison.

is compensated by a higher antenna gain. Varying S does not have a large influence on the amplitude and the shape of H_{Tx}. Looking only at $|S_{11}|$ and $|H_{Tx}|$ characteristics, one could say that the new directional antenna has a 20–30% lower bandwidth compared to the slot antenna. But the difference is not visible when looking at the transient results, when using the source pulse described earlier in Section II-B. Fig. 5(c) presents radiated waveforms by the omnidirectional slot antenna and the directional antenna with parameters as in Table I. We can see that the radiated pulses have almost the same shapes, but the electric field intensity is higher for directional antenna. Further investigations of the transient characteristics of both antennas are presented in more details in Section VII.

B. Variation of the Reflector Width

The return loss and the H_{Tx} of directional slot antenna, when varying values of the reflector width ($R_w = 8$, 12, 16 and 20 mm), were investigated. A decrease of impedance bandwidth, from 54% (3.7–6.4 GHz) for $R_w = 8$ mm, 47% (4–6.5 GHz) for $R_w = 16$ mm, to only 20% (5.3–6.5 GHz) when $R_w = 20$ mm was observed. Thus, considering only the impedance bandwidth, one would say that there is a significant difference when changing the reflector width. When considering H_{Tx}, however, we observed that its amplitude and shape is almost the same for different R_w values [similarly, as shown in Fig. 5(b)]. Based on the results from the previous

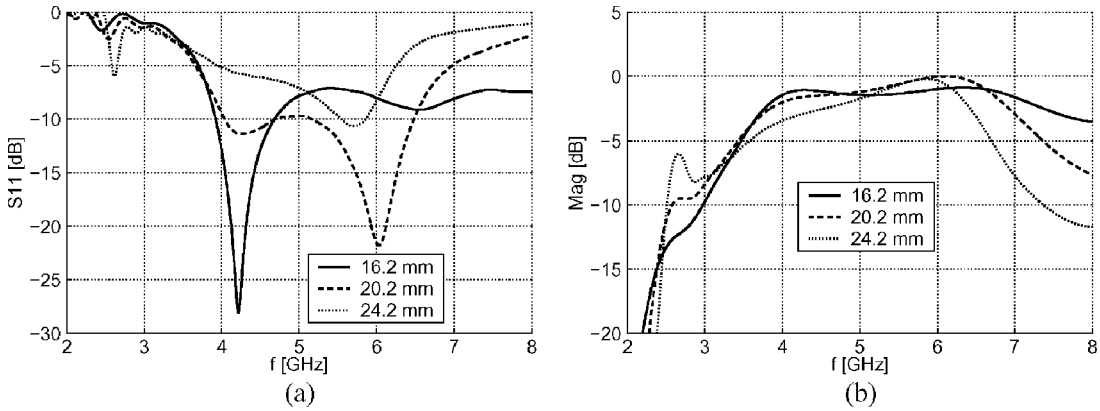

Fig. 7. (a) Return loss of the directional antenna for different ST values and (b) $|H_{Tx}(\omega, 0, 0)|$ for different ST values.

paragraph (Section II-A) of radiated pulses by antennas with different H_{Tx} characteristics, we could expect very similar pulses radiated from directional antennas with various R_w.

C. Variation of the Reflector Length

There is a certain *threshold* of the reflector length (R_l) resulting in a directive radiation characteristic. This length determines the lower frequency bound of antenna operation, in terms of directivity. To have F2B higher than 10 dB at 3.5 GHz this length is 36 mm. Parametric studies of the influence of the reflector length were done only for $R_l > 36$ mm (36, 40, 44, 48 mm). Above this length R_l does not affect significantly the $|S_{11}|$ and $|H_{Tx}|$ characteristics, indicating however a slight degradation in performance at the lower frequencies when shortening the reflector.

D. Variation of the Distance Between Feed Lines (ST)

Fig. 7 presents the influence of the spacing between parallel 100 Ω feed lines on characteristics of directional slot antenna. Results show that the distance between feed lines is one of the most critical parameters, for the impedance bandwidth and H_{Tx} characteristics. Position of the feed lines affects the field distribution in the slot. Therefore for a certain slot length there is an optimal value of ST, resulting in the widest impedance bandwidth, defining at the same time the characteristic of H_{Tx}. It should also be pointed out that to achieve the optimum bandwidth for a given ST value, the length of the tuning stubs (ST_{l1} and ST_{l2}) must be appropriately adapted. Note that for a different ST value there is also an optimum ST_{l1} and ST_{l2} value. No separate studies of varying ST_{l1} and ST_{l2} have been conducted.

E. Physical Operation of a Directional UWB Slot Antenna

To further investigate the physical operation of the new directional antenna, and the impact of the reflector on the antenna impedance and radiation, we have examined the near-fields of the antenna. In Fig. 8, we present the electric field distribution in a slot, for the antenna without [Fig. 8(a)] and with the reflector [Fig. 8(b)]. It can be seen that the reflector has a great influence on the field distribution at lower frequencies (3.5 and 4.5 GHz). At 6 GHz however, the field distribution is almost

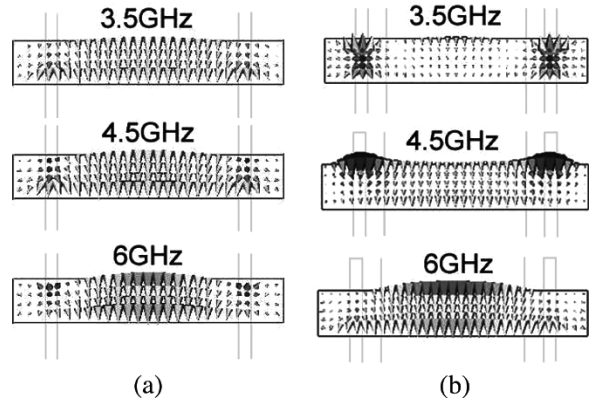

Fig. 8. Distribution of the electric field in the slot: (a) omnidirectional antenna and (b) directional antenna. Size of arrows corresponds to the field strength.

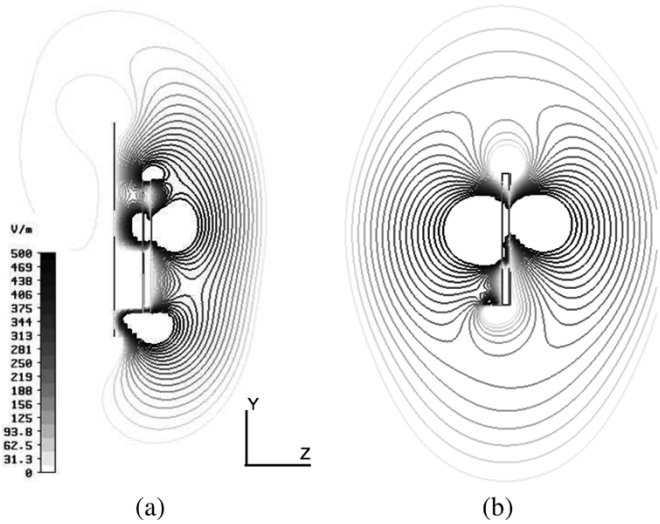

Fig. 9. Comparison of radiation mechanism at 4.5 GHz: (a) directional UWB slot antenna and (b) omnidirectional UWB slot antenna. Presented cut taken along the Y axis, at the center of the slot.

unchanged. This significant change in the field distribution especially at low frequencies explains the serious change in the return loss (impedance) between 3 and 5 GHz [see Fig. 5(a)].

Fig. 9 show the radiation of near-fields for the directional and omnidirectional slot antennas. Shown is the E_y field (co-polarization) component at 4.5 GHz, at a cut taken along the Y axis, at

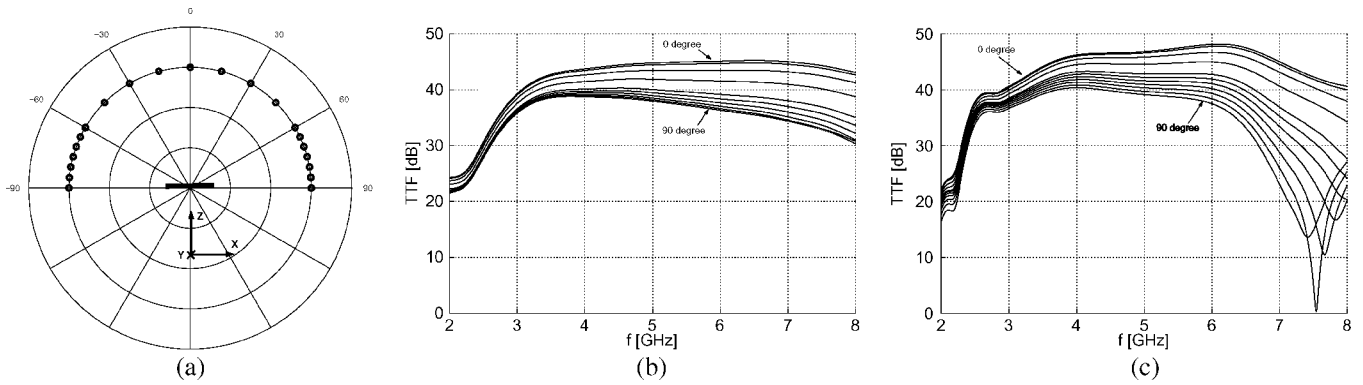

Fig. 10. (a) Placement of the time-domain probes (E_y far-field component). Transfer functions recorded along XZ plane for: (b) the omnidirectional slot antenna, and (c) the directional slot antenna with $R_w = 16$ mm.

the center of the slot (antenna symmetry axis). It is visible that the reflector function is a combination of radiation and reflection. From our observations of simple near-fields, we concluded that the reflector contributes more to the radiation process at the lower frequencies, and acts more as a simple reflector at the higher frequencies.

Additional prove of that comes when investigating the radiation phase center of antennas. We assume that the reference point ($x = 0$ mm, $y = 0$ mm, $z = 0$ mm) is placed in the center of the slot. Then, phase center of the omnidirectional antenna is at (0, −3.5, 2.8), (0, −3.5, 2.7) and (0, −3.5, 2.9) for 3.5, 4.5, and 6 GHz, respectively. So it practically does not move with frequency, what is very important for good transient behavior. The same calculation for the directional slot antenna (reflector at $z = -6$ mm) gives the phase centers located at (0, 0, −5.5), (0, 0, −3.4) and (0, 0, −2.8) for 3.5, 4.5, and 6 GHz, respectively. Therefore, we observe that with increasing frequency the phase center moves in the z direction closer and closer to that of the slot antenna without the reflector.

VI. Comparison of Antennas Operating in Free-Space

A. Spatially Averaged Transmit Transfer Functions

In the previously presented section we have studied the new directional antenna characteristics considering input matching, transmit transfer function, H_{Tx}, in the direction ($\theta = 0^\circ$, $\phi = 0^\circ$) and the radiation patterns at 3.5, 4.5, and 6 GHz. In this section we will present extended analysis of the two versions of directional UWB slot antennas, the omnidirectional UWB slot antenna and the monopole antenna (as a reference). As in the real application (WBAN) antenna should be as thin as possible, we have chosen two directional antennas, the first one with all parameters as in Table I, the second one with $R_w = 16$ mm. Investigations are based on the transient co-polarized electric (E_y) far-field signals (cross-polarization level ≤20 dB lower) from different directions in the upper hemi-sphere. A limited set of time-domain field values was chosen, along the XZ and YZ cuts. Locations are shown in Fig. 10(a). The number of points is higher for angles $60^\circ \le \theta \le 90^\circ$, to account for the higher pattern changes in these directions. For the calculations of H_{av} it gives $N = 11$ and $M = 4$ [see (3)]. From these probes we are able to characterize antennas in the time- and frequency-domain. In Fig. 10(b) and (c) we can see examples

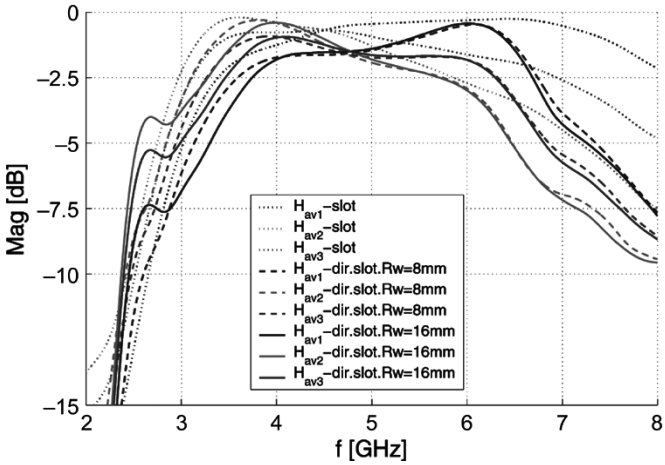

Fig. 11. Averaged transmit transfer functions for the slot antenna and the directional antennas with different reflector widths (8, 16 mm).

of transfer functions in XZ plane, for omnidirectional and directional $(R_w = 16$ mm) slot antennas. It should be noticed, that different slopes (positive, flat, negative) of transfer functions exist, depending on the angle of propagation. It means that within the limited frequency bandwidth the antenna will introduce angle-dependant time operators (e.g., derivation or integration) to the driving pulse.

Fig. 11 depicts the averaged transmit transfer functions (H_{av}) for all antennas. Three different H_{av} are calculated:

1. H_{av1}: H_{Tx} averaged over XZ and YZ planes, for θ angles between $0^\circ \le \theta \le 60^\circ$. This represents the radiation away from the human body, for body-mounted antenna.
2. H_{av2}: H_{Tx} averaged over XZ and YZ planes, for θ angles $60^\circ \le \theta \le 90^\circ$. This represents the radiation along the human body.
3. H_{av3}: H_{Tx} averaged over $0^\circ \le \theta \le 90^\circ$.

The directional slot antennas have a small difference in the averaged transfer functions for frequencies between 3 and 4 GHz. This difference is related to the input matching of these antennas. However the difference in the return loss characteristics of the slot antenna and directional slot antennas is not reflected in the H_{av} characteristics. On the other hand, for frequencies above 6.5 GHz we observe very different characteristics of H_{av} of the omnidirectional and the directional slot antennas, even if

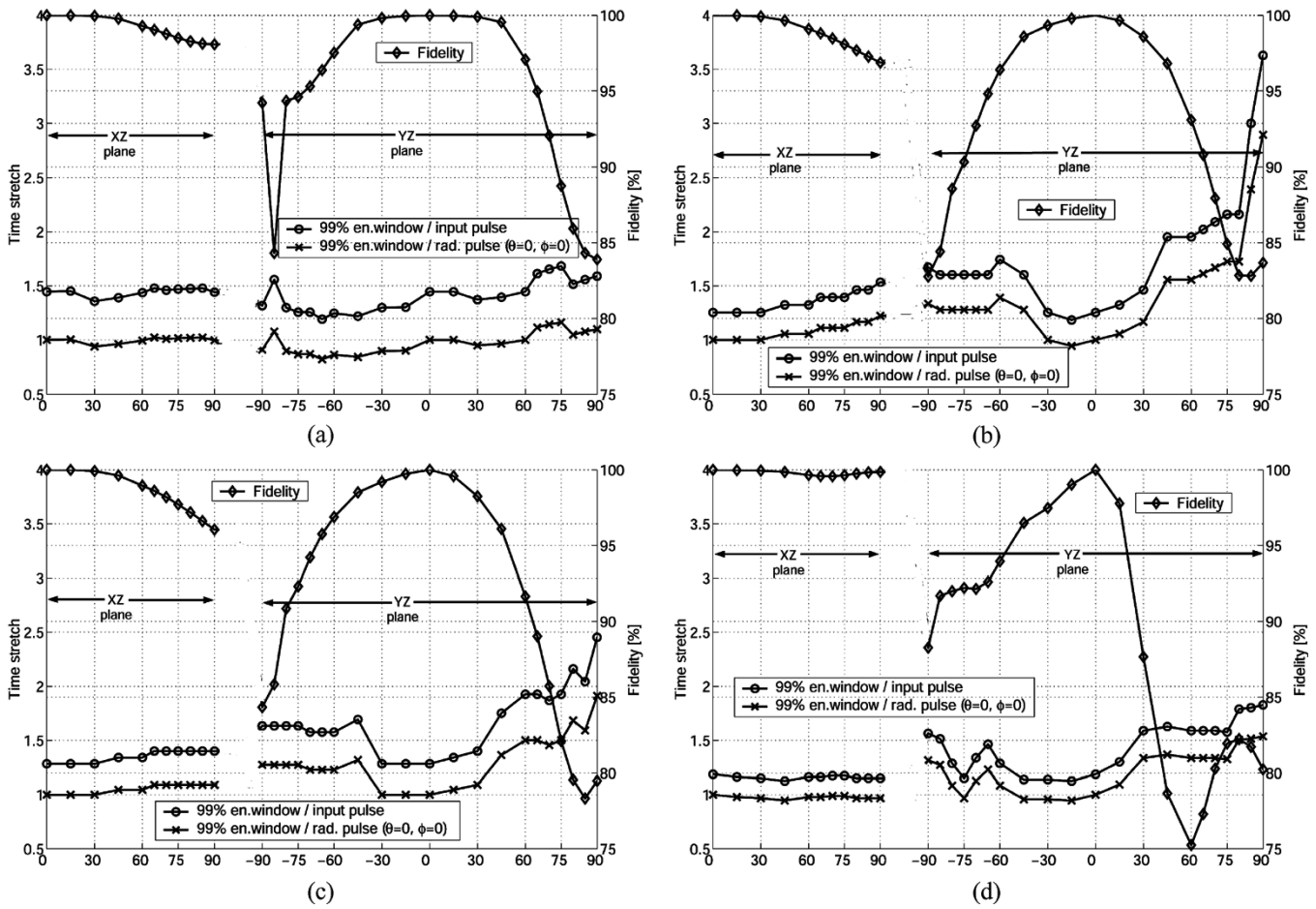

Fig. 12. Pulse distortion metrics for different antennas: (a) omnidirectional slot antenna, (b) directional slot antenna with $R_w = 8$ mm, (c) directional antenna with $R_w = 16$ mm, and (d) monopole antenna (as the reference).

their S_{11} characteristics look alike in this frequency range. It results from the fact that the gain of the directional antenna increases faster than for the omnidirectional slot antenna, thus its half-power beam width also decreases faster (from 71° at 3.5 GHz to 51° at 7 GHz, YZ plane) than for the omnidirectional slot antenna (from 80° at 3.5 GHz to 67° at 7 GHz, YZ plane). Therefore by choosing the 120° width of the solid angle for the H_{av1}, its amplitude drops above 6 GHz.

B. Pulse Distortion Parameters

Based on the H_{Tx} transfer functions we have calculated parameters showing quantitative angular characteristics of antennas for UWB systems: 1) 99% energy window (E99), relative to the input pulse; 2) 99% energy window, relative to the pulse radiated in the ($\theta = 0^\circ$, $\phi = 0^\circ$) direction; and 3) fidelity of radiated pulses (assuming the pulse radiated in ($\theta = 0^\circ$, $\phi = 0^\circ$) direction as the reference waveform). It should be noted that all these parameters depend on the pulse driving the antenna. Although these angular-dependent characteristics are very important from the point of view of UWB system design, they are very rarely presented in papers about antennas for UWB systems. Results are presented in Fig. 18. Driving pulse is the one presented in Section II-B. Results for the monopole antenna are presented for the reference.

The omnidirectional slot antenna has a fidelity above 98% in the XZ plane. In the YZ plane fidelity factors are above 95% for angles of θ between -70° and 65°, for the rest of considered directions F is lower, with a minimum of 84%. Very similar fidelity results are obtained for both directional slot antennas. There is a slight difference for the YZ plane, where $F > 95\%$ is for θ angles within $-65^\circ \div 50^\circ$. Monopole antenna has the fidelity above 99% in the XZ plane, but in the YZ plane it is much worse. $F > 95\%$ is only between -50° and 20°, and at 60° it reaches the minimum of 75%. Compared to all slot antennas, we can also notice asymmetry in the YZ plane, which results from the changes of radiation pattern for different frequencies. Considering pulse distortions based on time windows with 99% of the pulse energy (E99), we can see that directional antennas introduce higher spatial variations of the E99 time windows [Fig. 12(b) and (c)], compared to the slot antenna [Fig. 12(a)] and also to the monopole antenna [Fig. 12(d)]. Taking as the reference input antenna pulse (its E99 window is 0.392 ns), radiated pulses are 1.19–1.68 ($\Delta = 0.49$), 1.16–3.8 ($\Delta = 2.64$), 1.28–2.44 ($\Delta = 1.16$), 1.13–1.83 ($\Delta = 0.7$) times longer, for the slot antenna, directional slot antenna with $R_w = 8$ mm, directional slot antenna with $R_w = 16$ mm and monopole antenna, respectively. Angular spread of E99 windows is important if one is interested in applications where any relative position between Tx and Rx antennas is possible. An interesting point to notice that even if E99 windows are shorter

TABLE II
RADIATION EFFICIENCY (RAD.EFF.) AND PEAK SAR VALUES FOR THE DIRECTIONAL SLOT ANTENNA. INPUT POWER $P_{\text{in}} = 1$ W

3 layer body model / Muscle tissue						
	R_w=8 mm		R_w=16 mm			
Body-feed distance	7mm (1mm to the body)		7mm (1mm to the body)		10mm (4mm to the body)	
f[GHz]	Rad.Eff. [%]	SAR10g [W/kg]	Rad.Eff. [%]	SAR10g [W/kg]	Rad.Eff. [%]	SAR10g [W/kg]
3.5	47 / 56	7 / 6.7	56 / 65	4.6 / 3.8	68 / 77	2.6 / 1.9
4.5	53 / 73	8.4 / 6.6	65 / 81	5.6 / 3.3	80 / 92	2.5 / 1.3
6	75 / 87	6.1 / 3.9	85 / 92	3.1 / 2	91 / 95	1.7 / 1.9

TABLE III
RADIATION EFFICIENCY AND PEAK SAR VALUES FOR THE OMNI-DIRECTIONAL SLOT ANTENNA. INPUT POWER $P_{\text{in}} = 1$ W

3 layer body model / Muscle tissue						
Body-feed distance	2 mm (2 mm to the body)		7 mm (7 mm to the body)		10 mm (10 mm to the body)	
f[GHz]	Rad.Eff. [%]	SAR10g [W/kg]	Rad.Eff. [%]	SAR10g [W/kg]	Rad.Eff. [%]	SAR10g [W/kg]
3.5	12 / 6	24.6 / 25.1	36 / 47	14.7 / 11.9	48 / 65	11 / 7.4
4.5	7 / 15	27.7 / 27.3	40 / 64	17.3 / 10.4	56 / 77	11.9 / 6.1
6	27 / 29	21.8 / 28.9	64 / 76	11.5 / 7.7	78 / 85	6.7 / 4.5

between 45° and 75° of the YZ plane for the monopole than directional slot ($R_w = 8$ mm), its fidelity is lower at these directions. For the system considerations that would mean one would prefer a different antenna (directional slot or monopole), depending on the type of receiver (e.g., energy detector or template-based).

VII. COMPARISON OF ANTENNAS OPERATING CLOSE TO THE HUMAN BODY

To show the effect of the human body on the antenna characteristics we have simulated the same antennas as used in Section VII with the addition of the truncated human body models. For the different separations between the antenna and the body we have examined: antenna radiation efficiency, peak SAR values (10 g averaged), transmit transfer functions and input matching.

A. Radiation Efficiency and SAR

The objective of these investigations was to show the difference in the radiation efficiency and SAR values for different antennas. The slot antenna has the omnidirectional pattern (front-to-back ratio close to 0 dB) and the -10 dB impedance bandwidth within 3–6 GHz. The first directional slot antenna (reflector width $R_w = 8$ mm) has $|S_{11}| < -10$ dB within 3.7–6.4 GHz and power front-to-back ratio of 7.1, 7.4 and 11.7 dB at 3.5, 4.5, and 6 GHz, respectively. The second directional slot antenna (reflector width $R_w = 16$ mm) has the 10 dB return loss bandwidth within 4–6.5 GHz and power front-to-back ratio of 10.4, 10.8 and 15.4 dB at 3.5, 4.5, and 6 GHz, respectivel

y. For comparison we assume the same body-to-feed line distance, 7 and 10 mm. For directional slot antennas it means that the reflector is only 1 mm away from the body. Additional calculations were made for the omnidirectional slot antenna, when it was placed only 2 mm away from the body. The radiation efficiency and SAR values are presented in Table II for directional slot antennas and in Table III for the omnidirectional slot antenna. They show that:

- Radiation efficiency of all antennas increases with frequency. Only for the slot antenna in the position 2 mm away from the body was a different behavior observed.
- Antenna performance in terms of the radiation efficiency and SAR has improved for directional slot antennas, compared to the omnidirectional slot antenna.
- Comparing only directional slot antennas, better performance (radiation efficiency and SAR) was obtained for the one with wider reflector (16 mm). Therefore, one would choose different values of R_w for operation in free space than close to the human body.
- Comparing results obtained when using different body models, higher (than 4–24%) radiation efficiencies were calculated when homogeneous muscle-tissue body model was used. Again, different behavior for slot antenna 2 mm away from the body is observed. As the electrical parameters of skin and muscle tissue are very similar (conductivity plays a much bigger role than permittivity), the main difference between these two models is an incorporation of the fat tissue. Fat is a low water content tissue, thus its conductivity is lower than for skin and muscle.

As an illustration to the results presented in Table II and III we present the power absorbed in the skin layer (where the maximum absorption occurs) of the three-layer human body model. Fig. 13 shows results for the omnidirectional slot antenna, Fig. 14 for the directional slot antenna, normalized to the same absolute value. It is visible that with the use of reflector, near-fields where scattered, resulting in the lower power deposited in the tissue.

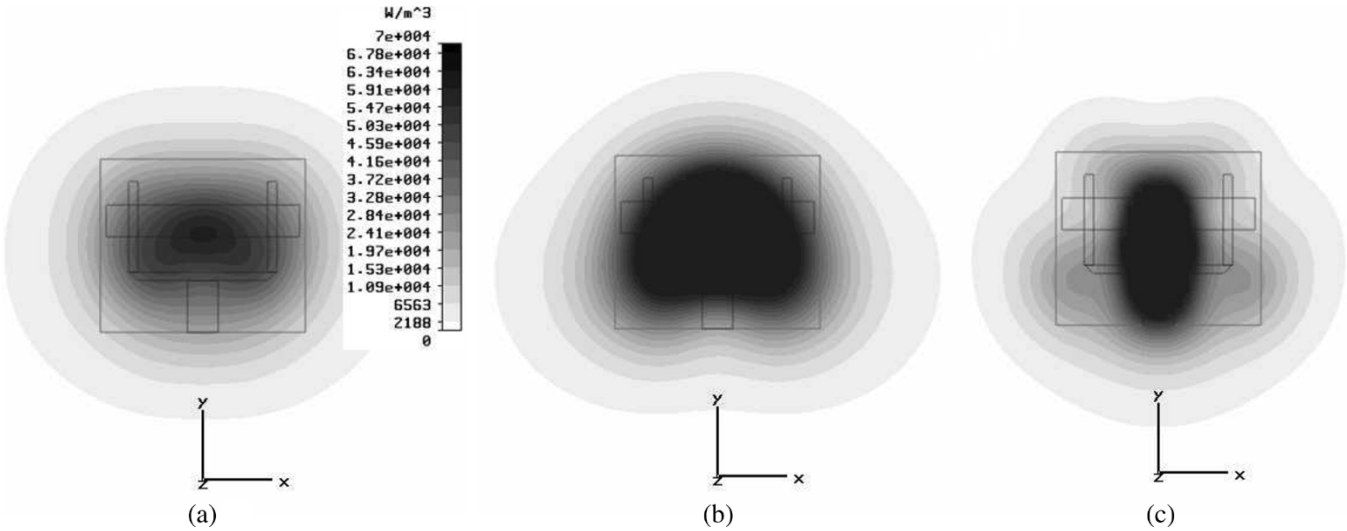

Fig. 13. Power absorbed in the skin layer of the three-layer human body model due to the omnidirectional slot antenna: (a) 3.5 GHz, (b) 4.5 GHz, and (c) 6 GHz. Distance between the skin and the feed-lines is 7 mm.

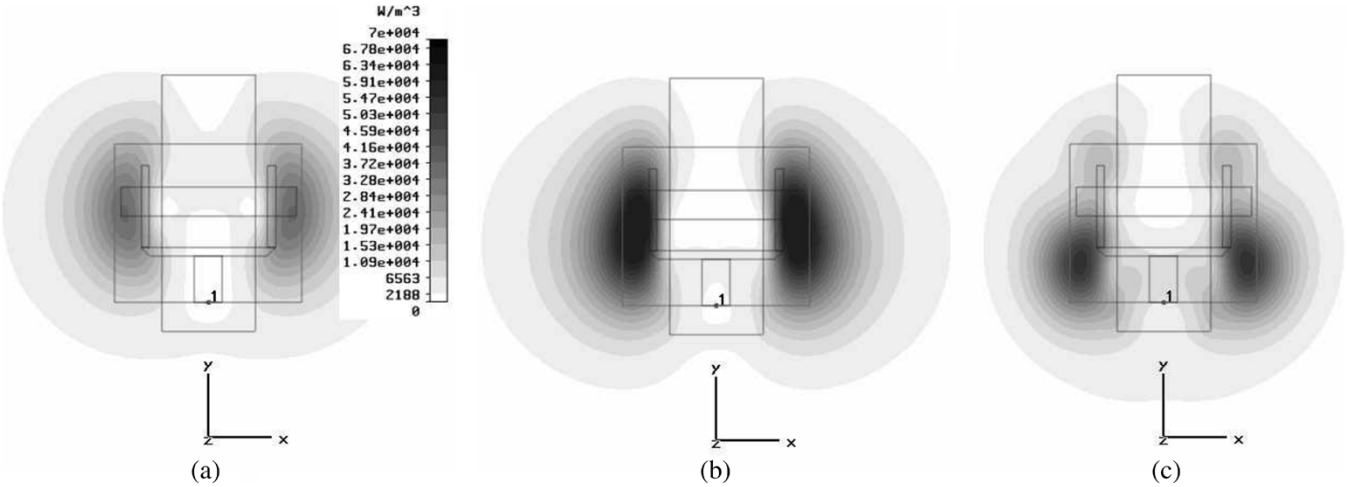

Fig. 14. Power absorbed in the skin layer of the three-layer human body model due to the directional slot antenna: (a) 3.5 GHz, (b) 4.5 GHz, and (c) 6 GHz. Distance between the skin and the feed-lines is 7 mm (1 mm between skin and reflector).

B. Averaged Transmit Transfer Functions and Impedance Bandwidth Characteristics

In Fig. 15 return loss characteristics of body-worn antennas are shown. The impedance bandwidth of the new directional antennas (for both R_w values, 8 and 16 mm) is almost the same when operating in a free space and close to the human body. The only noticeable difference exists for frequencies below 3.5 GHz, where the reflector element is not yet working properly and antennas have lower directivity (see Section VI-C). For the omnidirectional slot antenna, the impedance is greatly changed due to body proximity. However, because of losses in the human body, impedance bandwidth is preserved. Considering these facts, we may conclude that making the slot antenna directional results in a greatly decreased influence on the human body on its impedance. As for antennas operating in a free-space (see Fig. 11), we have calculated spatially averaged transmit transfer functions for body-worn antennas. Results are shown in Fig. 16(a). Transfer functions were averaged over the same solid angles as earlier (Section VII-A). In Fig. 16(b) the difference between H_{av} from the same solid angle when calculated for a free-space and body worn operational cases is presented.

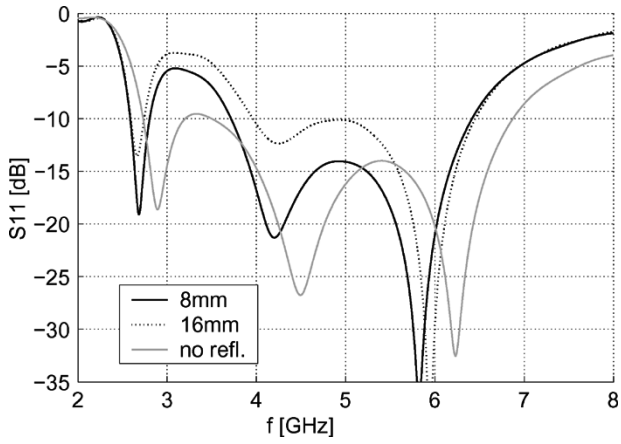

Fig. 15. Return loss of body-mounted antennas: new directional antennas with R_w of 8 and 16 mm, slot antenna. Body-feed line distance is 7 mm for all antennas.

We can clearly see that the new directional antennas are much less influenced by human body proximity, than the omnidirectional slot antenna. Results obtained for the directional antenna with reflector width of 16 mm are especially encouraging. The

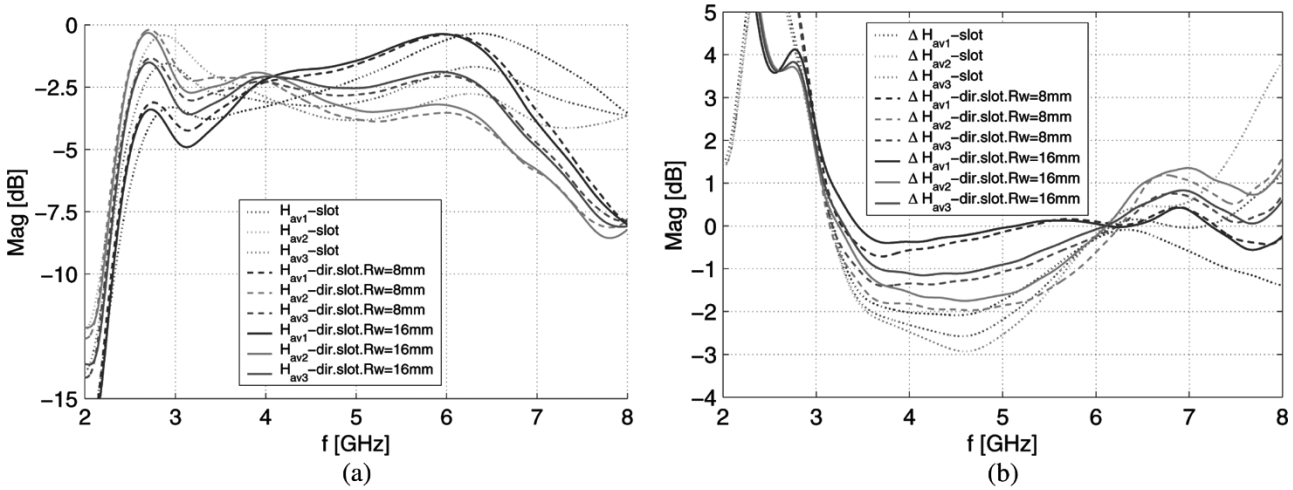

Fig. 16. (a) Spatially averaged transmit transfer functions (H_{av}) of body-mounted antennas: omnidirectional slot antenna and directional slot antennas with $R_w = 8$ and 16 mm: (b) Difference in H_{av} between free-space and body-mounted operations. Distance between feed line of antennas and the body is 7 mm.

H_{av1} transfer function (propagation from the body) within the 3.4–8 GHz band is maximally 0.5 dB different from the one in free-space. For the same frequency band, H_{av1} variations in the case of omnidirectional slot antenna are even up to 4 dB. Comparing only directional antennas, we can see again (as for the radiation efficiency and SAR), that the antenna with $R_w = 16$ mm performs slightly better, when one considers the difference in transient characteristics (H_{av}) between the free space and on the body operations.

VIII. Conclusion

A novel small-size directional UWB antenna for WPAN/WBAN applications has been proposed in this work. It utilizes the small reflecting/radiating patch element to achieve a front-to-back ratio above 10 dB in a very large bandwidth from 3.5 to 7 GHz. Antenna measurements with an optic RF setup were performed in order to characterize the small-size antenna far field radiation pattern. By means of numerical EM simulations, systematic parametric study was performed to understand the influence of the reflecting element on transient characteristics of the new antenna. As will be the case in normal WPAN/WBAN operating scenarios, antenna performance was examined when in free space and close to the human body. Two truncated body models were used, three-tissue model (skin, fat and muscle tissues) and homogeneous muscle tissue model. Performance of the novel directional UWB antenna was compared with the omnidirectional UWB slot antenna and with the UWB disc monopole antenna. As monopole antennas are very popular and commonly used in UWB systems, the latter one serves as the reference design.

In free space, spatial UWB characteristics of antennas have been obtained based on the transmit transfer functions, time windows with 99% energy and fidelity of radiated pulses. Results show that the new directional antenna has slightly larger values of 99% energy windows of radiated pulses compared to the UWB disc monopole. However, when considering fidelity of radiated pulses, the directional antenna performs better than the monopole, due to the more stable radiation pattern across the frequency band of interest. Therefore, our new design can be an attractive alternative to the popular UWB monopole antennas, especially for WBAN/WPAN applications where directional antenna could be of interest.

The advantage of using the proposed directional UWB antenna is even more pronounced if we consider its operation on the human body (UWB WBAN applications). Results show that for frequencies above 3.5 GHz, where the power front-to-back ratio of the directional antenna is greater than 10 dB, its impedance bandwidth is nearly the same as in the free space. It is not the case neither for the commonly used omnidirectional slot antenna nor monopole antennas. Furthermore, between 3 and 6 GHz the performance of the novel directional slot antenna, in terms of radiation efficiency and SAR, is significantly improved compared to omnidirectional antenna designs. Results of spatially averaged transfer functions also prove better performance of the directional slot antenna. They show that the difference of spatially averaged transfer functions between operation in the free space and when close to the body is much lower ($<$0.5 dB for H_{av1}, within 3.5–8 GHz) than for the omnidirectional slot antenna. These main observations lead to the conclusion that our new directional UWB antenna is indeed very suitable for UWB BAN applications, being a more efficient design with radiation characteristics less influenced by proximity of the human body.

References

[1] "European IST FP5 Project, Power Aware Communications for Wireless OptiMised Personal Area Networks (PACWOMAN)," http://www.imec.be/pacwoman, Oct. 2003.
[2] "European IST FP6 Project MAGNET," http://www.ist-magnet.org, Jan. 2004.
[3] "Human ++ Project," www.imec.be.
[4] T. Zasowski, F. Althaus, M. Staeger, A. Wittneben, and G. Troester, "UWB for noninvasive wireless body area networks: channel measurements and results," presented at the IEEE Conf. Ultra Wideband Systems and Technologies, UWBST, Reston, VA, Nov. 2003.
[5] Z. N. Chen, X. H. Wu, H. F. Li, N. Yang, and M. Y. W. Chia, "Considerations for source pulses and antennas in UWB radio systems," *IEEE Trans. Antennas Propag.*, vol. 52, no. 7, pp. 1739–1748, Jul. 2004.
[6] X. H. Wu and Z. N. Chen, "Design and optimization of UWB antennas by a powerful CAD tool: PULSE KIT," presented at the IEEE Antennas and Propag. Society Symp., Jun. 20–25, 2004.
[7] J. S. McLean, H. Foltz, and R. Sutton, "The effect of frequency-dependent radiation pattern on UWB antenna performance," presented at the Proc. IEEE Antennas and Propagation Society Symp., Jun. 20–25, 2004.

[8] H. G. Schantz, "Dispersion and UWB antennas," presented at the Proc. Joint Conf. Center For TeleInFrastruktur, Department of Communication Technology Int. Workshop Ultra Wideband Systems with Ultrawideband Systems and Technologies Conf., Kyoto, Japan, May 18–21, 2004.
[9] H. G. Schantz and L. Fullerton, "The diamond dipole: a Gaussian impulse antenna," presented at the IEEE Antennas and Propagation Soc. Symp., Jul. 8–13, 2001.
[10] M. Klemm and G. Troester, "Characterization of an aperture-stacked patch antenna for ultra-wideband wearable radio systems," in *Proc. 15th Int. Conf. Microwaves, Radar and Wireless Communications-MIKON*, vol. 2, Warsaw, Poland, May 17–19, 2004, pp. 395–398.
[11] D. H. Kwon and Y. Kim, "A small ceramic chip antenna for ultra-wideband systems," presented at the Int. Workshop on Ultra Wideband Systems Joint With Conf. Ultra Wideband Systems and Technologies, Kyoto, Japan, May 18–21, 2004.
[12] D. Manteuffel, J. Kunish, W. Simon, and M. Geissler, "Characterization of UWB antennas by their spatio-temporal transfer function based on FDTD simulations," presented at the Proc. EUROEM Conf., Magdeburg, Germany, Jul. 12–16, 2004.
[13] M. Klemm and G. Troester, "Small patch antennas for ultra-wideband wireless body area netwroks," presented at the EUROEM 2004 Conf., Magdeburg, Germany, Jul. 12–16, 2004.
[14] W. A. T. Kotterman, G. F. Pedersen, K. Olesen, and P. Eggers,, "Cableless measurement setup for wireless handheld terminals," in *Proc. Symp. Personal, Indoor and Mobile Radio Communications (PIMRC)*, vol. 1, Oct. 2001, pp. B112–B116.
[15] *Future Adaptive communication environment (FACE), internal research project*, Denmark: Center For PersonKommunikation Center for TeleInFrastruktur, Aalborg Univ., Mar. 2004.
[16] X. Qing and Z. N. Chen, "Antipodal vivaldi antenna for UWB applications," presented at the EUROEM 2004 Conf., Magdeburg, Germany, Jul. 12–16, 2004.
[17] A. G. Yarovoy, "Antenna development for UWB impulse radio," presented at the Eur. Microwave Week, Amsterdam, The Netherlands, Oct. 2004.
[18] W. S. T. Rowe and R. B. Waterhouse, "Reduction of backward radiation for CPW fed aperture stacked patch antennas on small ground planes," *IEEE Trans. Antennas Propag.*, vol. 51, no. 6, Jun. 2003.
[19] S. D. Targonski and D. M. Pozar, "Aperture-coupled microstrip antennas using reflector elements for wireless communications," in *Proc. IEEE-APS Conf. Antennas and Propagation for Wireless Communications*, Nov. 1998, pp. 163–166.
[20] D. Lamensdorf and L. Susman, "Baseband-pulse-antenna techniques," *IEEE Antennas Propag. Mag.*, vol. 36, no. 1, Feb. 1994.
[21] "Analysis for mean effective gain of mobile antennas in land mobile radio environments," *IEEE Trans. Veh. Technol.*, vol. 39, no. 2, May 1990.
[22] J. McLean, H. D. Foltz, and R. Sutton, "Pattern descriptors for UWB antennas," *IEEE Trans. Antennas Propag.*, vol. 53, no. 1, pp. 553–559, Jan. 2005.
[23] S. D. Targonski, R. B. Waterhouse, and D. M. Pozar, "Design of Wide-band aperture-stacked patch microstrip antennas," *IEEE Trans. Antennas Propag.*, vol. 46, no. 9, Sep. 1998.
[24] X. Qing, M. Y. W. Chia, and X. Wu, "Wide-slot antenna for UWB applications," in *Proc. IEEE Antennas and Propagation Soc. Int. Symp.*, vol. 1, Jun. 22–27, 2003, pp. 834–837.
[25] C. Gabriel, "Compilation of the dielectric properties of body tissues at RF and microwave frequencies,", AL/OE-TR-1996-0037 Rep., Jun. 1996.
[26] T.-Y. Shih, C.-L. Li, and C.-S. Lai, "Design of an UWB fully planar quasielliptic monopole antenna," presented at the Proc. Int. Conf. Electromagnetic Applications and Compatibility (ICEMAC 2004), Taipei, Taiwan, Oct. 14–16, 2004.

Maciej Klemm was born in 1978. He received the M.Sc. degree in microwave engineering from Gdansk University of Technology, Poland, in 2002.

In February 2003, he joined the Electronics Laboratory, Swiss Federal Institute of Technology (ETH) Zurich, Switzerland, where he is currently working toward the PhD. degree. In spring 2004, he was a visiting researcher at the Antennas and Propagation Laboratory, University of Aalborg, Denmark, where he was working on the new antennas for UWB radios. His current research interests include small UWB antennas and UWB communications, antenna interactions with a human body, electromagnetic simulations, microwave MCM technologies and millimeter-wave integrated passives (European IST LIPS project).

Mr. Klemm received a Best Paper Award at the IEEE MIKON May 2004 conference for a paper about antennas for UWB wearable radios.

István Z. Kovcs received the B.Sc. degree from "Politehnica" Technical University of Timisoara, Romania, in 1989, the M.Sc.E.E. degree from The Franco-Polish School of New Information and Communication Technologies/Ecole Nationale Supérieure des Télécommunications de Bretagne, Poland/France, in 1996, and the Ph.D.E.E. degree in wireless communications from Aalborg University, Aalborg, Denmark, in 2002.

Currently, he is holding the position of Assistant Research Professor with the Center For TeleInFrastruktur, Department of Communication Technology, Aalborg University, in the Antennas and Propagation Division. He is actively involved in the European IST PACWOMAN and IST MAGNET projects and participated in several industrial projects with partners such as TeleDanmark, Motorola, IOSpan, and ArrayComm. His research interests are in the field of radio channel propagation measurements and modeling, with major focus on short-range ultrawide-band radio channel and ultrawide-band antenna investigations.

Gert F. Pedersen was born in 1965. He received the B.Sc.E.E. degree from the College of Technology, Dublin, Ireland, and the M.Sc.E.E. degree from Aalborg University, Aalborg, Denmark, in 1993.

Since 1993 he was employed by Aalborg University, Department of Communication Technology, where he is currently working within the Center For TeleInFrastruktur as an Associate Research Professor heading an antenna group. His research has focused on radio communication for mobile terminal, including antennas, diversity systems, propagation and biological effects. He has also worked as a Consultant for developments of antennas for mobile terminals including the first internal antenna for mobile phones in 1994 with very low SAR, first internal triple-band antenna in 1998 with low SAR and high efficiency, smallest internal dual-band antenna in 2000, and various antenna diversity systems rated as the most efficient on the market. Recently, he has been involved in establishing a method to measure the communication performance for mobile terminals that can be used as a basis for a 3G standard where measurements also including the antenna will be needed. Further, he is involved in mobile terminals for 3G including several antennas to enhance the data communication.

Gerhard Tröster (SM'93) received the M.S. degree from the Technical University of Karlsruhe, Karlsruhe, Germany, in 1978 and the Ph.D degree from the Technical University of Darmstadt, Darmstadt, Germany, in 1984, both in electrical engineering.

He is a Professor and Head of the Electronics Laboratory, ETH Zürich, Zürich,Switzerland. During the eight years he spent at Telefunken Corporation, Germany, he was responsible for various national and international research projects focused on key components for ISDN and digital mobile phones. In 1997, he cofounded the spinoff u-blox ag. He authored and coauthored more than 100 articles and holds five patents. His field of research includes wearable computing, reconfigurable systems, signal processing, mechatronics, and electronic packaging.